Wind and Structures, Vol. 1, No. 1 (1998) 43-57
DOI: http://dx.doi.org/10.12989/was.1998.1.1.043

Wind-induced coupled translational-torsional motion of tall buildings

S. Thepmongkorn† and K.C.S. Kwok‡

Department of Civil Engineering, The University of Sydney, NSW 2006, Australia

Abstract. A three-degree-of-freedom base hinged assembly (BHA) for aeroelastic model tests of tall building was developed. The integral parts of a BHA, which consists of two perpendicular plane frames and a flexural pivot, enable this modelling technique to independently simulate building translational and torsional degree-of-freedom. A program of wind tunnel aeroelastic model tests of the CAARC standard tall building was conducted with emphasis on the effect of (a) torsional motion, (b) cross-wind/torsional frequency ratio and (c) the presence of an eccentricity between centre of mass and centre of stiffness on wind-induced response characteristics. The experimental results highlight the significant effect of coupled translational-torsional motion and the effect of eccentricity between centre of mass and centre of stiffness on the resultant rms acceleration responses in both along-wind and cross-wind directions especially at operating reduced wind velocities close to a critical value of 10. In addition, it was found that the vortex shedding process remains the main excitation mechanism in cross-wind direction even in case of tall buildings with coupled translational-torsional motion and with eccentricity.

Key words: tall buildings; coupled motion; aeroelastic modelling technique; cross-wind/torsional frequency ratio; eccentricity; wind-excitation mechanisms.

1. Introduction

Recent advances in the use of high strength materials, innovative structural system, structural analysis methodology and efficient construction methods, have increased the number of taller and more slender buildings and towers with a wide variety of shapes all over the world. The major design consideration for this new generation of tall buildings is wind-induced forces and responses, in particular the resultant acceleration response which affects occupant comfort and is a critical factor in the design process. In the case of tall buildings which have an eccentricity between centre of mass and centre of stiffness, i.e., tall buildings which have asymmetric stiffness distribution in plan, or ones with complex geometrical shapes such as cut-outs and/or multiple level of set-backs, not only the two translational degree-of-freedom but also torsional degree-of-freedom are of major concern. The resultant responses, which are coupled translationally and torsionally, may be greatly amplified at the corner region of the building. Analytical studies of wind-induced coupled translational-torsional motion of tall buildings have been performed and the importance of the coupling between translational and torsional motion have been recognised, e.g., Patrickson and Friedmann (1979), Tallin and Ellingwood (1985) and Kareem (1985). However, a comprehensive study of wind-induced coupled motion and wind-excitation mechanism is limited

† Ph.D. Student
‡ Associate Professor

due to lack of the relevant information from wind tunnel aeroelastic model tests.

This paper presents the experimental results from wind tunnel model tests of the CAARC (Commonwealth Advisory Aeronautical Research Council) standard tall building with coupled translational-torsional motion in order to provide a better understanding of wind-induced response characteristics and wind-excitation mechanisms.

2. Base hinged assembly technique

Base hinged assembly (BHA) for aeroelastic modelling of tall buildings was originated by Kwok, *et al.* (1994) in 1994. The basic concept of this modelling technique is the simulation of

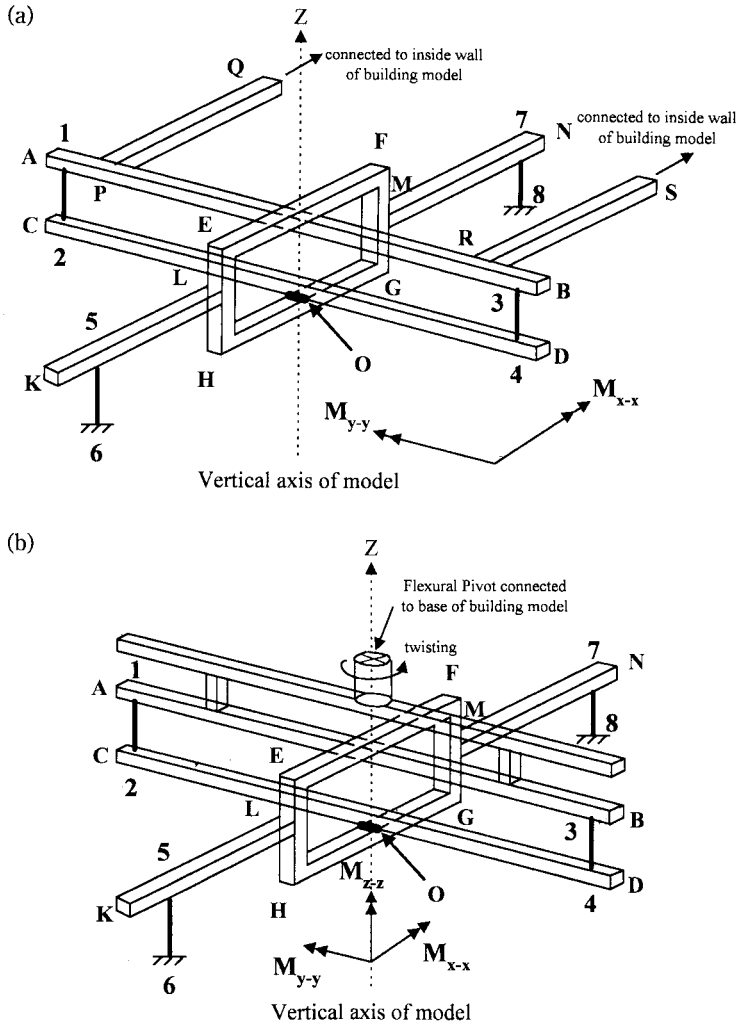

Fig. 1 Base hinged assembly test rig : (a) two-degree-of-freedom system; (b) three-degree-of-freedom system. – AB and CD are rigid members aligned in the same vertical planes. – EFGH is a rigid rectangular frame, GH is attached to bottom of CD while EF runs above and perpendicular to AB. – KL and MN are rigid members attached to frame EFGH. – PQ and RS are rigid members attached to AB. – 1-2 and 3-4 are flexural elements designed to examine the overturning moment $M_{y\text{-}y}$. – 5-6 and 7-8 are flexural elements designed to examine the overturning moment $M_{x\text{-}x}$

the building stiffness using two perpendicular plane frames. The original configuration of a BHA is shown in Fig. 1*a* in which ABCD and KLMN are two perpendicular plane frames rigidly connected to each other at point O. The integral parts of each frame are flexural elements, i.e., 1-2, 3-4, 5-6 and 7-8, which are specially designed to match the stiffness of the building model in its two principal directions. Consequently, the use of two perpendicular sets of flexural elements allows the simulation of building translational degree-of-freedom in two directions to be completely independent. The base of the rigid timber model of a tall building is attached to a BHA at point Q and S, forming a BHA model.

Further development and refinement of a BHA model to determine the full capacity and limitations of this modelling technique have been ongoing since late 1996. Thepmongkorn, *et al.* (1997) employed a BHA to examine wind-induced response characteristics of the CAARC standard tall building. The study program included an investigation of the effect of stiffness of flexural elements on frequencies of model, integration of an oil damper to provide the variation of damping of the system and investigation of response characteristics under various wind conditions. It was found that the frequencies of vibration of a BHA model can be accurately predicted by a free-standing-cantilever model. In addition, the results from the wind tunnel model tests indicated that the responses of the CAARC building in along-wind and cross-wind directions, for reduced velocities ranging from 3 to 20, observed by a BHA model are similar to those observed by a conventional stick model and other published records. The major advantages of a BHA model are its simplicity and its ability to readily change the mass, stiffness, structural damping and geometric of building model. Two perpendicular frames of a BHA provide the ability to independently simulate building translational degree-of-freedom in its two principal directions and the ability to be further developed to model coupled translational-torsional motion.

A new generation of a BHA, which incorporates two translational and one torsional degree-of-freedom, is shown in Fig. 1*b*. In this case, a cantilevered Bendix flexural pivot was introduced to a BHA to provide a torsional degree-of-freedom. This flexural pivot is a frictionless bearing of limited angular travel which requires no lubrication.

3. Base hinged aeroelastic model

The rectangular prismatic shape CAARC standard tall building as shown in Fig. 2 was selected for a detailed study. The building corresponds to a prototype width, D_x, 30 m, length, D_y, 45 m, height, H, 180 m and building density, ρ_s, 160 kg/m^3. The subject building has linear sway mode shapes and a structural damping value, ξ, of 0.01 in both directions. Natural frequencies of the building were selected as variable parameters for a study of the effect of coupled translational-torsional motion on wind-induced response characteristics.

An aeroelastic model and balance system, as shown in Fig. 3, was used in this study. A 1:400 scaled timber model of the CAARC building was attached to a BHA by a screwed connection by which the base of the model can be adjusted to the desired level along the vertical axis to provide the best approximation of the true sway mode shapes. The eccentricities e_x and e_y of the building model can be physically modelled by offsetting the vertical axis of a flexural pivot, which coincides with the vertical axis of a BHA, to match them in each directions. This can be achieved by adjusting the centriod of the top plate of a BHA as shown in Fig. 3. Finally, a simple oil damper was attached to the bottom corner of the model below the wind tunnel floor to provide the variation of damping of the system.

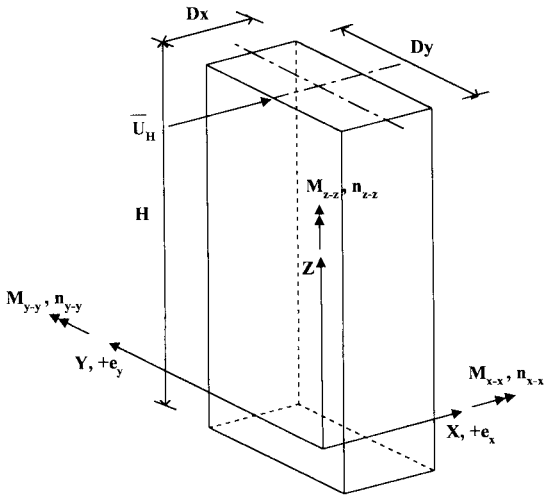

Fig. 2 CAARC building model and notations

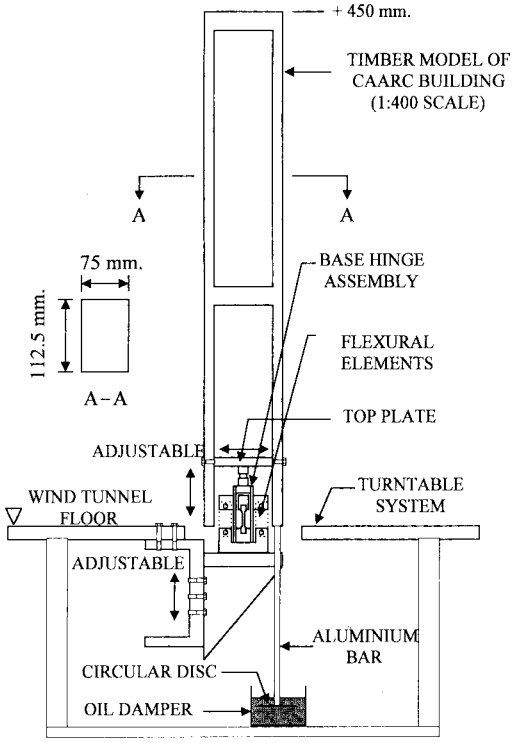

Fig. 3 Base hinged aeroelastic model and balance system

4. Experimental program

Wind tunnel tests of the BHA model were performed in a boundary layer wind tunnel in the Fluids Laboratory, University of Sydney. A natural wind model corresponding to an open terrain (AS1170.2-1989), with a power law exponent of the mean wind speed profile $\alpha \cong 0.15$ and a turbulence intensity at top of the building model $I_u \cong 0.10$, was simulated using a set of spires

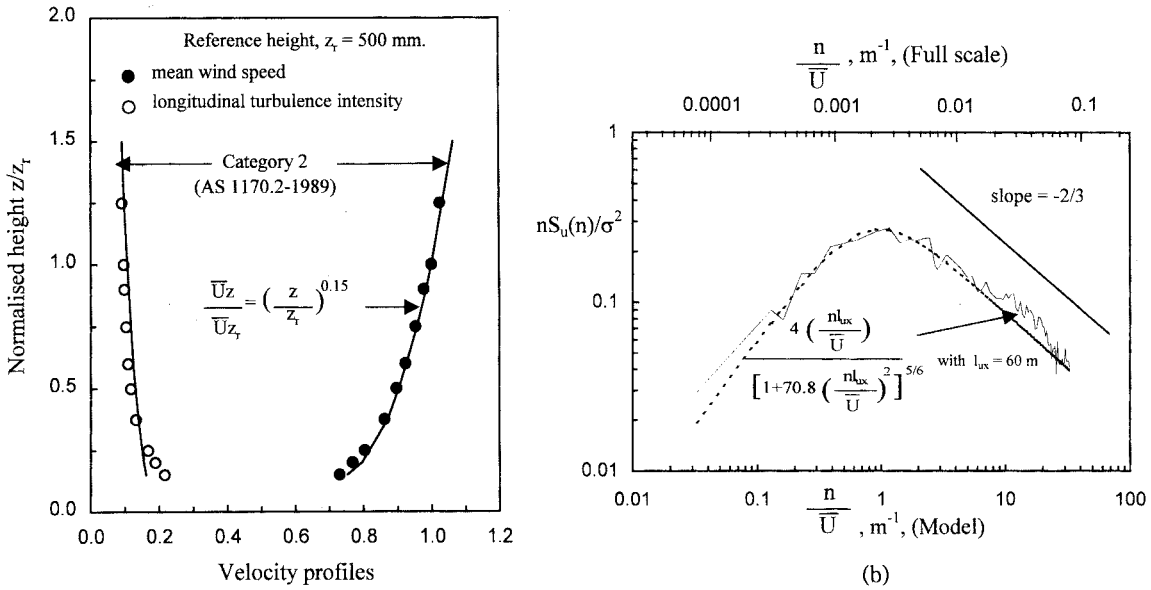

Fig. 4 Characteristics of a natural wind model : (a) mean wind speed and longitudinal turbulence intensity profiles; (b) longitudinal velocity spectrum at top of the model

and roughness elements placed upstream of the working section of the wind tunnel. The characteristics of the simulated wind, i.e., mean wind speed profile, turbulence intensity profile and longitudinal velocity spectrum of wind speed at top of the building model, were measured using a linearlised DISA hot-wire anemometer and the results are presented in Fig. 4.

Three accelerometers were located at the top of the CAARC standard tall building model in order to investigate the effect of coupled translational-torsional motion and structural eccentricity on wind-induced response characteristics. Two accelerometers were located at point A and B, which are 40 mm apart from each other, to sense the acceleration of the building model in y direction, $\ddot{y}_a$ and $\ddot{y}_b$ and another accelerometer was located at point C to measure the acceleration in x direction, $\ddot{x}$, as shown in Fig. 5. It was assumed that the acceleration caused by torsional motion manifested as the translational acceleration when the angle of rotation is small, therefore the translational acceleration $\ddot{x}$ and $\ddot{y}_a$ were used as an indicator of wind-induced response characteristics and discussions were made based on these two accelerations.

An experimental program to examine the effect of (a) torsional motion, (b) cross-wind/torsional frequency ratio and (c) the presence of an eccentricity between centre of mass and centre of stiffness on wind-induced response characteristics, were performed in the boundary layer wind tunnel. Six test cases as shown in Table 1 were carried out and the results were presented in the next section.

Free vibration tests were conducted at the beginning of the wind tunnel tests to confirm natural frequency and damping of a scaled aeroelastic model. The effect of coupled translational-torsional motion on the natural frequency, $n_{x\text{-}x}$ and $n_{y\text{-}y}$, and damping, $\zeta_{x\text{-}x}$ and $\zeta_{y\text{-}y}$, of a BHA model, were also investigated. It was found that coupled translational-torsional motion significantly decreased the natural frequency, $n_{x\text{-}x}$ and $n_{y\text{-}y}$, by approximately 24% and 20% respectively, as shown in Table 1. However, it was also found that coupled translational-torsional motion has a negligible effect on the damping, $\zeta_{x\text{-}x}$ and $\zeta_{y\text{-}y}$, of the model.

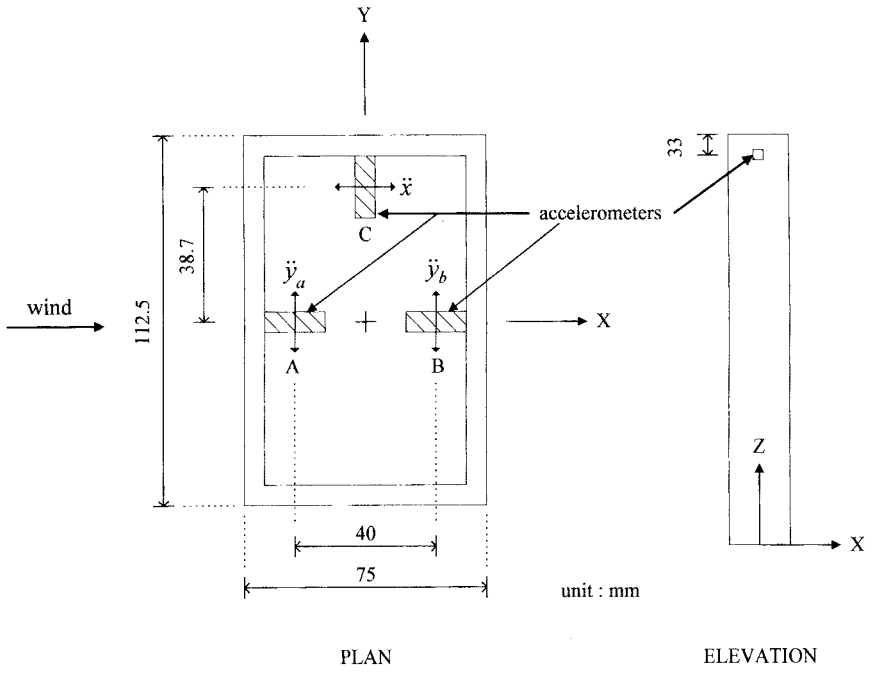

Fig. 5 Arrangement of accelerometers at top of the model

Table 1 Summary of experimental test cases

Case	$n_{x\text{-}x}$ (Hz)	$n_{y\text{-}y}$ (Hz)	$n_{z\text{-}z}$ (Hz)	$n_{x\text{-}x}/n_{z\text{-}z}$	e_x (mm)	e_y (mm)	e_x/D_x (%)	e_y/D_y (%)
1	4.04	4.35	∞	–	0	0	0	0
2	3.33 (4.04)	3.96 (4.35)	5.54	0.60	0	0	0	0
3	4.68 (5.80)	3.64 (4.35)	5.54	0.84	0	0	0	0
4	4.68 (5.80)	3.64 (4.35)	5.54	0.84	+10	0	+13.3	0
5	4.68 (5.80)	3.64 (4.35)	5.54	0.84	+10	-10	+13.3	-8.9
6	4.68 (5.80)	3.64 (4.35)	5.54	0.84	0	-10	0	-8.9

Note : $n_{x\text{-}x}$, $n_{y\text{-}y}$ and $n_{z\text{-}z}$ listed in the table are frequency of the building model about x, y and z axes respectively, obtained from free vibration tests when it is undergoing coupled translational-torsional motion, while the number listed in the parentheses are the frequency of the model when it independently vibrates about x and y axes.

The decrease in the natural frequency of the CAARC building model is believed to be caused by the effect of the coupling between translational and torsional degree-of-freedom, which caused changes in the equation of motion of the system. This effect can be readily illustrated by the analytical study of a three-degree-of-freedom single mass model as shown in an Appendix A. In this case, torsional degree-of-freedom, θ, of the rigid block creates the translational degree-of-

freedom, x_2 and y_2, which is coupled with the original translational degree-of-freedom, x_1 and y_1. By introducing a degree of coupling parameter, c, i.e., $x_2=cx_1$ and $y_2=cy_1$, the equation of motion of the system can be formulated and presented in a generalised form as seen by Eqs. (A5) and (A6). In fact, the degree of coupling parameter, c, can be varied from zero (uncoupled) to one (fully coupled) depended upon the closeness of the natural frequency in torsional and translational modes. The analytical results indicated that, for the CAARC building with fully coupled mode, the natural frequencies $n_{x\text{-}x}$ and $n_{y\text{-}y}$ can be decreased by up to 44% and 22% depended on the stiffness ratio k_3/k_2 and k_3/k_1, as shown in Fig. A3*b* and A3*a* respectively.

The maximum decrease in $n_{x\text{-}x}$ and $n_{y\text{-}y}$ by approximately 24% and 20%, respectively, observed in this study, indicated a high degree of coupling due to the closeness of the natural frequency in torsional and translational modes as shown in Table 1. Furthermore, the experimental results indicated little effect of coupled motion on the damping, $\zeta_{x\text{-}x}$ and $\zeta_{y\text{-}y}$, of the model and this observation is consistent with the analytical prediction as seen by Eqs. (A5*c*) and (A6*c*) respectively.

5. Response characteristics

The resultant rms accelerations at point C, $\sigma_{\ddot{x}}$ and point A, $\sigma_{\ddot{y}_a}$, in case of the incident wind normal to the wide face of the building model, are plotted as a function of reduced velocity, $\bar{U}_H/(n_{x\text{-}x}.D_y)$ and presented in Figs. 6 and 7. It should be noted that a specific term "resultant acceleration" is used to represent the acceleration, which contains both translational component caused by translational motion and torsional component caused by torsional motion.

Coupled translational-torsional motion has a significant effect on both the along-wind resultant rms acceleration, $\sigma_{\ddot{x}}$, and cross-wind resultant rms acceleration, $\sigma_{\ddot{y}_a}$, as shown in Figs. 6*a*

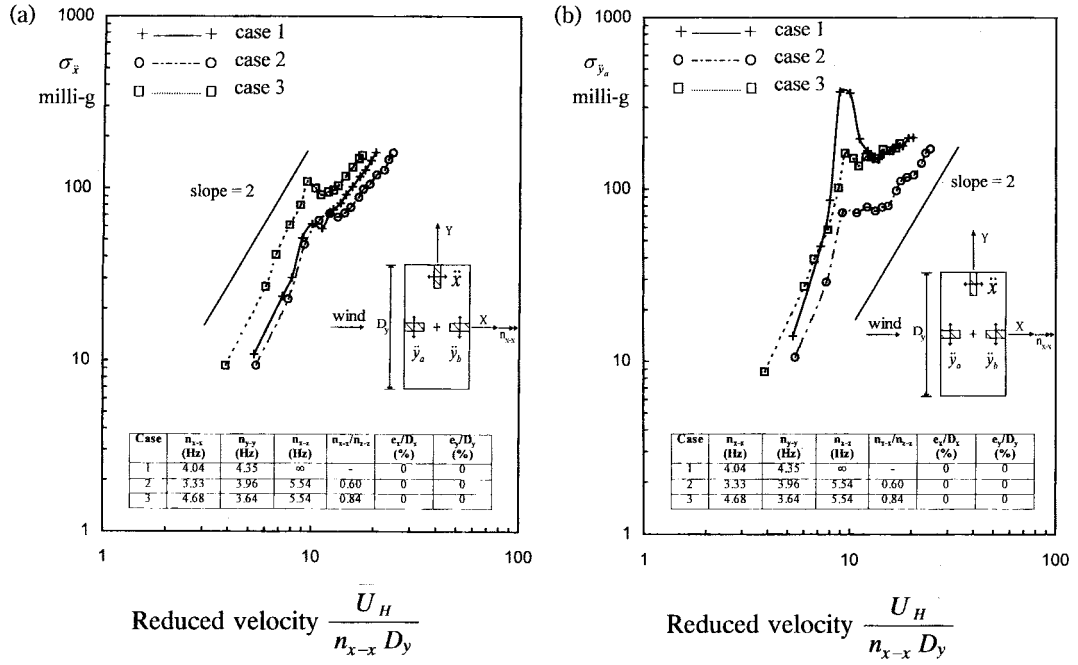

Case	$n_{x\text{-}x}$ (Hz)	$n_{y\text{-}y}$ (Hz)	$n_{t\text{-}t}$ (Hz)	$n_{x\text{-}x}/n_{t\text{-}t}$	e_x/D_x (%)	e_y/D_y (%)
1	4.04	4.35	∞	-	0	0
2	3.33	3.96	5.54	0.60	0	0
3	4.68	3.64	5.54	0.84	0	0

Fig. 6 Resultant rms acceleration at top of the CAARC building model as a function of reduced velocity at structural damping 0.01 for different cross-wind/torsional frequency ratio : (a) along-wind response, $\sigma_{\ddot{x}}$; (b) cross-wind response, $\sigma_{\ddot{y}_a}$

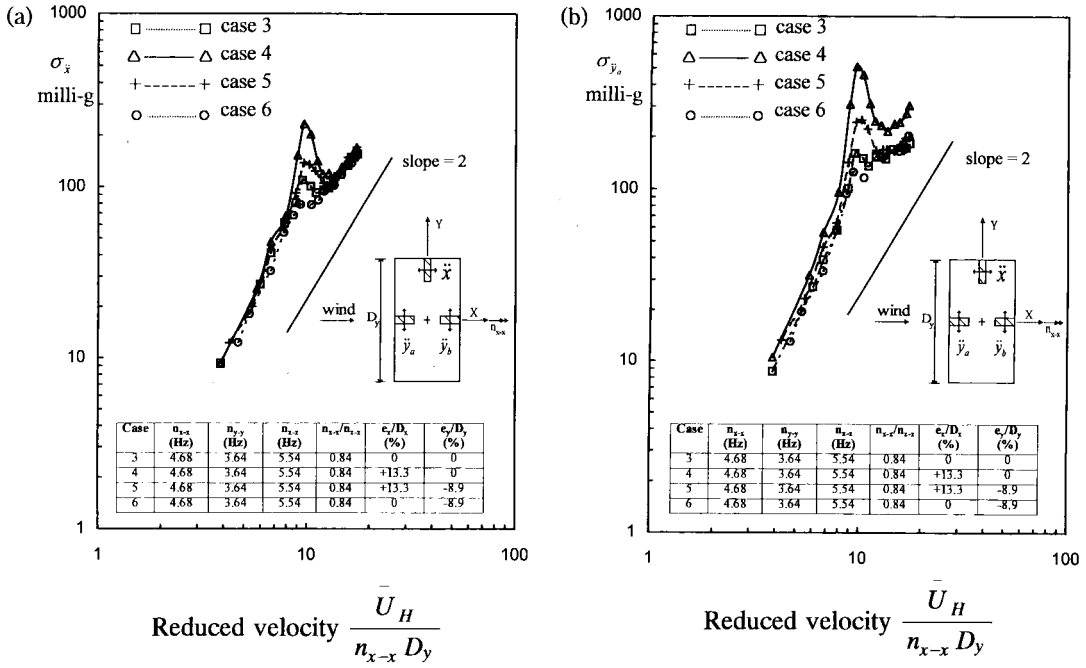

Fig. 7 Resultant rms acceleration at top of the CAARC building model as a function of reduced velocity at structural damping 0.01 for different eccentricity : (a) along-wind response, $\sigma_{\ddot{x}}$; (b) cross-wind response, $\sigma_{\ddot{y}_a}$

and 6*b*, of which the main findings can be summarised as :

(a) For reduced velocities ranging from 4 to 8 :
Coupled motion decreased the along-wind response, $\sigma_{\ddot{x}}$, in the test Case 2 (cross-wind/torsional frequency ratio 0.60), by approximately 15% and cross-wind response, $\sigma_{\ddot{y}_a}$, by approximately 35%. However, when the frequencies of vibration in cross-wind and torsional directions approach each other, which corresponds to the test Case 3 (cross-wind/torsional frequency ratio 0.84), coupled motion affected the responses by increasing the along-wind, $\sigma_{\ddot{x}}$, and cross-wind, $\sigma_{\ddot{y}_a}$, responses by approximately 80% and 20% respectively.

(b) For reduced velocities ranging from 8 to 12 :
A significant reduction in the cross-wind response, $\sigma_{\ddot{y}_a}$, by approximately 80% and 60% at operating reduced velocities close to a critical value of 10 was observed in the test Case 2 and Case 3 respectively. At operating reduced velocities close to a critical value of 10, a more prominent peak in the along-wind response, $\sigma_{\ddot{x}}$, is evident in the test Case 3. This is believed to be caused by oscillation energy transferred from cross-wind direction to along-wind direction through torsional motion, particularly when cross-wind/torsional frequency ratio approaches unity.

(c) For reduced velocities higher than 12 :
Coupled motion decreased the along-wind, $\sigma_{\ddot{x}}$, and cross-wind, $\sigma_{\ddot{y}_a}$, responses in Case 2 by approximately 20% and 40% respectively. However for Case 3, coupled motion increased the along-wind response, $\sigma_{\ddot{x}}$, by approximately 15%, while the cross-wind response, $\sigma_{\ddot{y}_a}$, was essentially unchanged.

It is evident that, for reduced velocities ranging from 4 to 20, coupled motion has a significant effect on both the along-wind, $\sigma_{\ddot{x}}$, and cross-wind, $\sigma_{\ddot{y}_a}$, responses. When the cross-wind

frequency is well below the torsional frequency, for example at a cross-wind/torsional frequency ratio of 0.60, coupled motion decreased both the along-wind, $\sigma_{\ddot{x}}$, and cross-wind, $\sigma_{\ddot{y}_a}$, responses. However, when the frequencies of vibration in cross-wind and torsional directions approach each other, such as when cross-wind/torsional frequency ratio was 0.84, an increase in the responses, particularly the along-wind response, $\sigma_{\ddot{x}}$, due to coupled translational-torsional motion was evident. However, at operating reduced velocities close to a critical value of 10, coupled motion significantly decreased the cross-wind responses, $\sigma_{\ddot{y}_a}$, in both Case 2 and Case 3. These effects of coupled motion and cross-wind/torsional frequency ratio will have a significant impact on the estimation of cross-wind response of tall buildings.

The effects of eccentricity between centre of mass and centre of stiffness on wind-induced response characteristics of the CAARC building model with coupled translational-torsional motion are shown in Fig. 7. It is evident that eccentricity has a significant effect on both the along-wind, $\sigma_{\ddot{x}}$, and cross-wind, $\sigma_{\ddot{y}_a}$, responses, in particular at operating reduced velocities close to a critical value of 10. For Case 4 in particular, where the eccentricity was shift to 10 mm downwind (13.33% of the building width), both the along-wind, $\sigma_{\ddot{x}}$, and cross-wind, $\sigma_{\ddot{y}_a}$, responses were substantially increased. In this case, the cross-wind response, $\sigma_{\ddot{y}_a}$, was greatly increased by approximately 240% and part of the energy of vibration was apparently transferred to the along-wind direction and significantly increased the along-wind response, $\sigma_{\ddot{x}}$, by approximately 110%. It is interesting to note that all rms response curves in Figs. 7*a* and 7*b* showed the same characteristic, the only difference is their magnitudes, especially at operating reduced velocities close to a critical value of 10. It is, therefore, believed that the wind-excitation mechanisms in each case are the same.

6. Wake spectrum

The most common sources of cross-wind excitation for most tall buildings is associated with vortex shedding and is frequently referred to as wake excitation. In this study, the investigation of wake characteristic, in particular frequency distribution, around an oscillating body was conducted in order to estimate the energy contribution due to the vortex shedding process.

Velocity fluctuations in a near wake of the CAARC building model were measured by a linearlised DISA hot-wire anemometer, which is the most common type of instrumentation used in the investigation of this nature. According to Kwok (1977), the hot-wire was located just outside the wake region to avoid the effect of flow reversals, but close enough to detect the frequency of velocity fluctuations due to periodic vortex shedding wakes. A measuring height of 75% of the building height, where the flow was not expected to be affected by flow entrainment from the top of the building, was selected. Two wind velocities were selected for a detailed study, the first one corresponds to the reduced velocity well below 10 and another one is close to a critical value of 10. Four cases, which emphasise the effect of the eccentricity on wind-induced coupled translational-torsional motion, were tested in the wind tunnel.

Wake spectra of the CAARC building model with 0.01 critical damping in an open terrain wind environment at reduced velocities of 5.75 and 9.65 are shown in Figs. 8 and 9 respectively. Longitudinal velocity spectra of the upstream wind measured at top of the model are also shown in the figure as dotted lines for comparison.

The wake spectra provide a reasonable representation of the energy available in the wake and assessment will be made mainly in terms of frequency distribution of this energy. The energy of velocity fluctuations in the wake is concentrated at the reduced frequency of about 0.1 for all

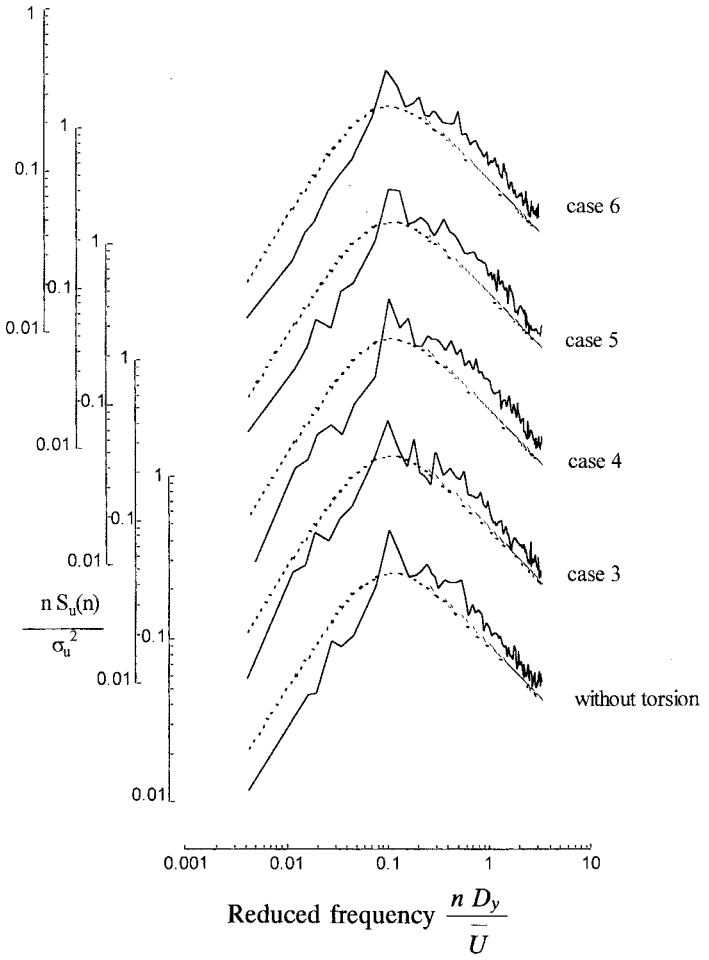

Fig. 8 Wake spectra of the CAARC building model at structural damping 0.01 and reduced velocity 5.75.

cases, including that for the building without torsional motion, as can be seen in Figs. 8 and 9. The peak of the wake spectra at the reduced frequency of 0.1 is consistent with the concentrated excitation energy associated with the vortex shedding process, which is a common wind-excitation mechanisms of tall buildings without coupled translational-torsional motion and with sharp edges. This characteristic has been widely reported by many researchers, e.g., Melbourne (1975), Bearman and Davies (1975), Kwok and Melbourne (1981) and Kwok, *et al.* (1988). It can be concluded that the vortex shedding process remains the main excitation mechanism in cross-wind direction even in case of tall buildings with coupled translational-torsional motion. In addition, it is evident from Figs. 8 and 9 that there is a narrowing and an increase in the magnitude of the spectral peak when the vortex shedding frequency and the natural frequency is close together, that is at operating reduced velocities close to a critical value of 10. This increase in magnitude of the spectral peak is expected to be accompanied by a corresponding increase in the cross-wind force spectrum, which was reported by Kwok, *et al.* (1988) and resulted in an increase in the cross-wind response. The spectral peak in building Case 4 with eccentricity is the highest and this resulted in the largest cross-wind acceleration response compared with other cases, as shown in Fig. 7*b*.

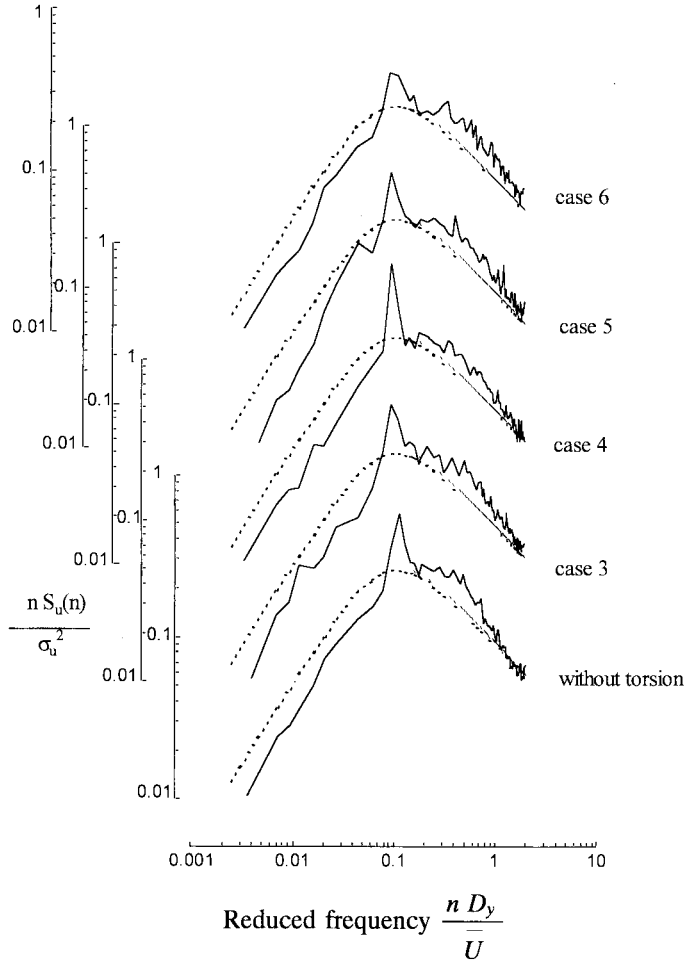

Fig. 9 Wake spectra of the CAARC building model at structural damping 0.01 and reduced velocity 9.65

7. Conclusions

A three-degree-of-freedom base hinged assembly for aeroelastic model tests of tall buildings was developed. The modelling technique has the ability to independently simulate building translational and torsional degree-of-freedom by using two perpendicular plane frames and a flexural pivot.

Aeroelastic model tests of the CAARC standard tall building were performed in a boundary layer wind tunnel in the Fluids Laboratory, University of Sydney. Six test cases were carried out to examine the effect of (a) torsional motion, (b) cross-wind/torsional frequency ratio and (c) the presence of an eccentricity between centre of mass and centre of stiffness on wind-induced response characteristics. The experimental results indicated the significant effect of coupled translational-torsional motion on both the along-wind and cross-wind rms acceleration responses at reduced velocities ranging from 4 to 20. For the CAARC building model with a cross-wind/torsional frequency ratio of 0.60, coupled motion decreased both the along-wind and cross-wind rms acceleration responses. However, when cross-wind/torsional frequency ratio approaches unity, an increase in the rms acceleration response was evident. In particular, an increase in the along-wind rms acceleration response by up to 80% was found at operating reduced velocities lower than 10.

In addition, at operating reduced velocities close to a critical value of 10, a large decrease in cross-wind rms acceleration response was observed in both cases of cross-wind/torsional frequency ratio and a decrease by up to 80% was found when cross-wind/torsional frequency ratio was 0.60. Therefore, it is evident that cross-wind/torsional frequency ratio has a significant effect on wind-induced response characteristics, and this effect warrants further studies.

The effect of an eccentricity between centre of mass and centre of stiffness on wind-induced coupled translational-torsional motion was also investigated. The eccentricities tend to increase both the along-wind and cross-wind rms responses. The responses tend to vary with the degree of eccentricity and an increase in cross-wind rms responses by approximately 240% has been observed where the centre of stiffness was shifted to $0.13D_x$ downwind. However, from the analysis of wake energy distribution, it was found that the vortex shedding process remains the main excitation mechanism in cross-wind direction even in cases of tall buildings with coupled translational-torsional motion and with eccentricity.

Acknowledgements

The authors acknowledge the contribution of Dr. Lakshmanan of Structural Engineering Research Centre, Madras, who pioneered the base hinged assembly concept and assisted in its development since 1994. The financial support from Mahanakorn University of Technology (MUT), Thailand is gratefully acknowledged. The authors wish to thank Messrs. Mark MacLean, Steve Johnson and Pong Li, Technical Officers of the Department of Civil Engineering, University of Sydney for the construction of a prototype BHA and a timber model of the CAARC building.

References

Bearman, P.W. and Davies, M.E. (1975), "The flow about oscillating bluff structures", *Proceedings of the 4th International Conference on Wind Effects on Buildings and Structures*, Cambridge University Press, September, 285-295.

Kareem, A. (1985), "Lateral-torsional motion of tall buildings to wind loads", *Journal of Structural Engineering* **111**(11) 2479-2496.

Kwok, K.C.S. (1977), "Cross-wind response of structures due to displacement dependent excitations", thesis presented to the Department of Mechanical Engineering, Monash University, at Victoria, Australia, in fulfilment of the requirements for the degree of Doctor of Philosophy, 155-163.

Kwok, K.C.S. and Melbourne, W.H. (1981), "Wind-induced lock-in excitation of tall structures", *Journal of the Structural Division ASCE* **107**(ST1) 57-72.

Kwok, K.C.S., Wilhelm, P.A. and Wilkie, B.G. (1988), "Effect of edge configuration on wind-induced response of tall buildings", *Engineering Structures* **10** 135-140.

Kwok, K.C.S., Lakshmanan, N. and Donovan, P.F. (1994), "Development of a special base hinge assembly for stick models", *Report PROJ.UNDP/IND/91/011*, Structural Engineering Research Centre, Madras, India, December.

Melbourne, W.H. (1975), "Cross-wind response of structures to wind action", *Proceedings of the 4th International Conference on Wind Effects on Buildings and Structures*, Cambridge University Press, September, 343-358.

Patrickson, C.P. and Friedmann, P.P. (1979), "Deterministic torsional building response to winds", *Journal of the Structural Division ASCE* **105**(ST12) 2621-2637.

Standards Australia, *SAA Loading Code Part 2 : Wind Loads*, AS1170.2-1989.

Tallin, A. and Ellingwood, B. (1985), "Wind induced lateral-torsional motion of buildings", *Journal of Structural Engineering* **111**(10) 2197-2213.

Thepmongkorn, S., Kwok, K.C.S. and Lakshmanan, N. (1997), "A two-degree-of-freedom base hinged aeroelastic (BHA) model for response predictions", Volume of Abstracts, *4th Asia-Pacific Symposium*

on Wind Engineering, Gold Coast, Australia, July, 239-242.

Appendix A-Three-degree-of-freedom single mass model

In a three-degree-of-freedom single mass model as shown in Fig. A1, mass, elastic resistance to displacement and energy-loss mechanism, are represented by : mass (m); mass moment of inertia (I_m); stiffness (k_1, k_2, k_3); and damping (c_1, c_2, c_3) respectively. The x_1 and y_1 translational degree-of-freedom resulting from translational motion and the x_2 and y_2 translational degree-of-freedom resulting from torsional motion, are assumed created by the wind. The system is represented by the inertia f_I, damping f_D and elastic spring force f_S, as shown in Fig. A1*b*. Since x_1 and y_1 are independent, it is more appropriate to formulate the equation of motion in each direction independently.

Consider now the motion of the rigid block in x-direction as shown in Fig. A2, the inertia f_I, damping f_D and elastic spring force f_S, are given by : $f_{S1}=k_1x_1$; $f_{D1}=c_1\dot{x}_1$; $f_{I1}=m\ddot{x}_1$; $f_{S3}=k_3\theta$; $f_{D3}=c_3\dot{\theta}$

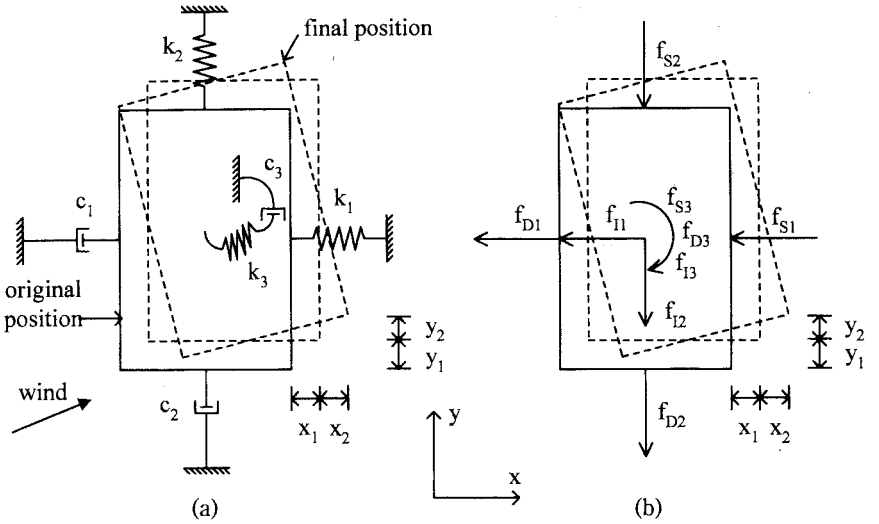

Fig. A1 Three-degree-of-freedom single mass system : (a) basic components; (b) resisting force components

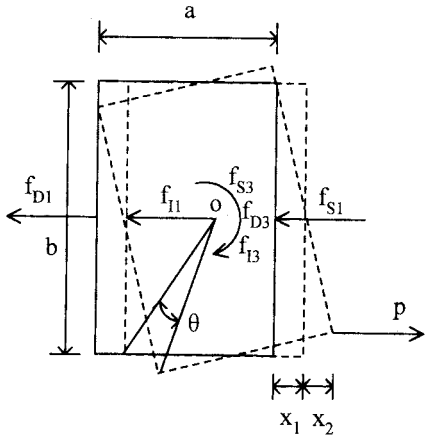

Fig. A2 x-θ coupled motion

and $f_{I3}=I_m\ddot{\theta}$. The equilibrium equations, $\Sigma F_x=0$ and $\Sigma M_o=0$, are given by :

$$m\ddot{x}_1+c_1\dot{x}_1+k_1x_1=p \tag{A1}$$

$$I_m\ddot{\theta}+c_3\dot{\theta}+k_3\theta=\frac{pb}{2} \tag{A2}$$

where the dots represent differentiation with respect to time. In case x_1 and θ are uncoupled, Eqs. (A1) and (A2) give two separated circular frequencies of vibration, i.e., $\omega_1=2\pi n_1=\sqrt{k_1/m}$ and $\omega_3=2\pi n_3=\sqrt{k_3/I_m}$. However, if x_1 and θ become coupled, Eqs. (A1) and (A2) have to be solved simultaneously, thus

$$m\ddot{x}_1+\frac{2}{b}I_m\ddot{\theta}+c_1\dot{x}_1+\frac{2}{b}c_3\dot{\theta}+k_1x_1+\frac{2}{b}k_3\theta=2p \tag{A3}$$

Substituting $I_m=m\dfrac{a^2+b^2}{12}$; $\theta=\dfrac{2}{b}x_2$; $\dot{\theta}=\dfrac{2}{b}\dot{x}_2$ and $\ddot{\theta}=\dfrac{2}{b}\ddot{x}_2$ into Eq. (A3), gives

$$m\ddot{x}_1+\frac{a^2+b^2}{3b^2}m\ddot{x}_2+c_1\dot{x}_1+\frac{4}{b^2}c_3\dot{x}_2+k_1x_1+\frac{4}{b^2}k_3x_2=2p \tag{A4}$$

Introducing a degree of coupling parameter, c, i.e., $x_2=cx_1$ and rewrites Eq. (A4) as :

$$m_1^*\ddot{x}_1+c_1^*\dot{x}_1+k_1^*x_1=p_1^* \tag{A5a}$$

in which $m_1^*=\left(1+\dfrac{a^2+b^2}{3b^2}c\right)\cdot m$ = generalised mass (A5b)

$$c_1^*=\left(1+\frac{4}{b^2}\frac{c_3}{c_1}c\right)\cdot c_1 \quad \text{= generalised damping} \tag{A5c}$$

$$k_1^*=\left(1+\frac{4}{b^2}\frac{k_3}{k_1}c\right)\cdot k_1 \quad \text{= generalised stiffness} \tag{A5d}$$

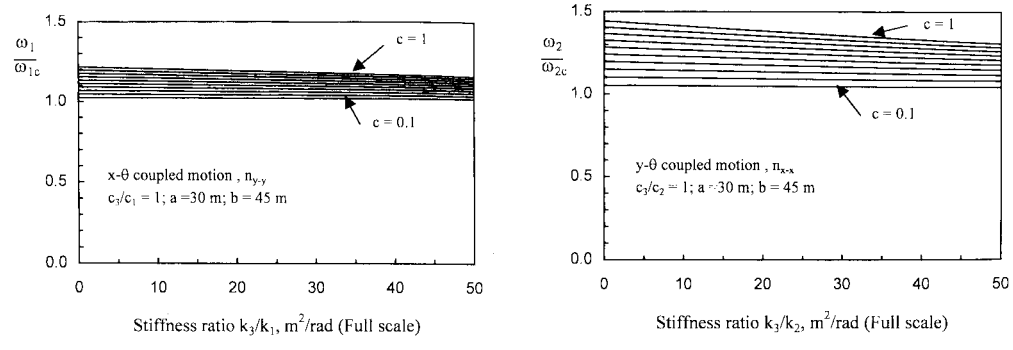

(a) (b)

Fig. A3 Variation of a frequency ratio as a function of stiffness ratio for the CAARC building with coupled translational-torsional motion : (a) x-θ coupled motion; (b) y-θ coupled motion

$$p^*_1 = 2p \qquad = \text{generalised load} \tag{A5e}$$

Eqs. (A5 *a-e*) give the generalised form of the coupled x-θ equation of motion in which the circular frequency of vibration is given by $\omega_{1c} = 2\pi n_{1c} = \sqrt{k^*_1/m^*_1}$. The plot of the uncoupled/coupled frequency ratio, ω_1/ω_{1c}, as a function of stiffness ratio, k_3/k_1, for the CAARC building (a=30 m and b=45 m) is shown in Fig. A3*a*.

The coupled y-θ equation of motion can be formulated in the same fashion and the generalised form is given by :

$$m^*_2 \ddot{y}_1 + c^*_2 \dot{y}_1 + k^*_2 y_1 = p^*_2 \tag{A6a}$$

in which $m^*_2 = \left(1 + \frac{a^2+b^2}{3a^2} c\right) \cdot m$ = generalised mass (A6b)

$$c^*_2 = \left(1 + \frac{4}{a^2}\frac{c_3}{c_2} c\right) \cdot c_2 \quad = \text{generalised damping} \tag{A6c}$$

$$k^*_2 = \left(1 + \frac{4}{a^2}\frac{k_3}{k_2} c\right) \cdot k_2 \quad = \text{generalised stiffness} \tag{A6d}$$

$$p^*_2 = 2p \qquad = \text{generalised load} \tag{A6e}$$

Finally, the circular frequency of vibration is given by $\omega_{2c} = 2\pi n_{2c} = \sqrt{k^*_2/m^*_2}$ and the variation of the uncoupled/coupled frequency ratio, ω_2/ω_{2c}, as a function of stiffness ratio, k_3/k_2, for the CAARC building (a=30 m and b=45 m) is shown in Fig. A3*b*.

It is evident that the frequencies of vibration in both directions were decreased by the influence of coupled motion, which depend on the degree of coupling, c, as shown in Fig. A3. It was also found that, in case c_1=c_2=c_3 and c=1, Eqs. (A5*c*) and (A6*c*) give the ratio $c_1/c^*_1 \cong 1.00$ and $c_2/c^*_2 \cong 1.00$, which indicate a negligible effect of coupled motion on damping of the system.